PERGAMON

Deep-Sea Research I 45 (1998) 1393–1410

DEEP-SEA RESEARCH
PART I

Short-term variability of the underwater light field in the oligotrophic ocean in response to surface waves and clouds

Malgorzata Stramska[a,*], Tommy D. Dickey[b]

[a] *University of Southern California, Hancock Institute for Marine Studies, Los Angeles, CA 90089-0373, USA*
[b] *ICESS, University of California at Santa Barbara, Santa Barbara, CA 93106-3060, USA*

Received 17 March 1997; received in revised form 16 January 1998; Accepted 17 February 1998

Abstract

Examples of short-term variations of the underwater light field associated with surface-wave focusing and cloud cover, and occurring at intermediate depths of the euphotic zone in the oligotrophic ocean are discussed. Time series of water pressure, spectral downwelling irradiance (E_d), and spectral upwelling radiance (L_u) at 412, 443, 490, 510, 555, 665, and 683 nm were acquired with moored instruments. The mooring was deployed in the Sargasso Sea near Bermuda in September 1994. The measurements were made at 15 and 35 m once every hour from 6 a.m. to 8 p.m. local time, with a 6 Hz sampling rate over time periods of 2 or 5 min duration. Time series of E_d, L_u, and water pressure were subject to spectral analysis. Under clear sky conditions, the power spectra of E_d at the blue/green wavelengths exhibited distinct maxima due to focusing of sunlight by surface waves. These maxima were located at a frequency higher than the dominant frequency in the power spectrum of water pressure variations. Similar maxima were present in the power spectra of L_u, but the position of the peak was dependent on light wavelength. The coefficient of variation for E_d and L_u depended on light wavelength and increased towards the red wavelengths. This coefficient was much smaller for L_u than for E_d, which reflects the fact that the upwelling light field is less affected by wave focusing than the downwelling light field. At depths of our measurements, the light fluctuations in the red can be attributed to variations in inelastically scattered radiation, that is, the fluorescence of phytoplankton cells and Raman scattering. This is because the fluoresced light and Raman scattered light in the red follow fluctuations that occur at shorter excitation wavelengths. When clouds covered the sky, we observed a decrease of the coefficient of variation for E_d and L_u. In this case, the fluctuations of light were well correlated with variations of water pressure associated with water surface displacement due to the wave motion.

* Corresponding author. Tel.: 001 213 740 0901; e-mail: stramska@usc.edu

0967-0637/98/$ - see front matter
PII: S0967-0637(98)00020-X

1. Introduction

Among the most characteristic features of the underwater light field are intense time variations, which include slower changes occurring on seasonal, synoptic, and diurnal time scales as well as within-day short-term fluctuations on the order of hours, minutes, and fractions of a second (e.g. Kirk, 1994). The dominant sources of the short-term variability are clouds and surface waves. The extent and type of cloud cover are of great importance in determining the amount of solar energy incident on the sea surface and penetrating into the ocean. For example, a layer of stratus clouds may transmit only about 10% of solar radiation. In the case of broken cloud cover, the incoming irradiance at the sea surface is intermittently varying from high to low values as clouds pass through the observing area. In recent years a large amount of new information on the effects of clouds on the spatial and temporal variability of solar irradiance around the Earth has become available from satellite remote sensing (e.g., Bishop and Rossow, 1991).

Under sunny sky conditions, strong fluctuations in downwelling irradiance (E_d) are attributed to focusing and defocusing of sunlight rays refracted by surface waves (e.g., Schenck, 1957; Dera and Gordon, 1968; Snyder and Dera, 1970; Nikolaev et al., 1972). The irradiance pulses caused by wave focusing can exceed the time average values of E_d by as much as 5-fold at shallow depths under a wind-disturbed sea surface (Dera and Stramski, 1986). Because of the geometrical nature of the focusing phenomenon and because of the light scattering within the water, the intensity of wave focusing effects decreases rapidly with depth, accompanied by the shift of dominant frequencies of fluctuations toward lower frequencies. Wave-induced fluctuations of underwater irradiance also result from variations in water column height above the light collector. As the significant components of the wave spectrum propagate, the surface moves up and down about the mean sea level, and the light is attenuated over a fluctuating pathlength. This type of wave-induced light fluctuation propagates throughout the entire euphotic zone, and the associated variance of E_d is greatest at frequencies corresponding to the most energetic range of the surface wave spectrum. The fluctuations caused by variations in the water column height are expected to dominate total E_d variance under completely diffuse irradiation of the sea surface when the sky is covered with clouds.

Understanding of underwater light field variability is important for designing *in situ* experiments based on optical techniques. For example, the effects of surface waves on the underwater light field can lead to errors in traditional estimates of the vertical attenuation coefficient (K_d) (Weidemann et al., 1990). While in traditional measurements wave-induced fluctuations of E_d represent an undesired noise, in another approach the high temporal resolution time series of E_d and water pressure were used to derive K_d from a single fixed-depth instrument (Stramski et al., 1992). The success of this method is based on the assumption that the dominant source of the E_d fluctuations are the changes in water column height above the light collector. Other sources of light variability, for example light fluctuations due to focusing effects, must be negligibly small for this approach to work well. Better understanding of relationships between the dominant sources of irradiance fluctuations and their statistical properties is needed for optimization of this method.

The underwater light field variability may also be of significance for various photochemical processes in the ocean. For example, radiant flux penetrating into the water controls the growth and cellular physiology of phytoplankton. It is well known that the photosynthetic rate depends not only on the amount of radiative energy received by the plants, but also on the manner in which the radiation is received (Thornley, 1974; Gross and Chabot, 1979; Gross, 1982). In the past there has been an increased interest in phytoplankton responses to within-day variations in the natural light regime (Marra, 1978; Gallegos et al., 1980; Abbott et al., 1982; Marra and Heinemann, 1982). Several experiments investigated responses of phytoplankton to the high-frequency light fluctuations induced by sea-surface waves. A decrease in carbon assimilation rate was observed by Dera et al. (1975). Lower, higher, or unchanged photosynthetic rates in fluctuating light as compared to constant light were observed in other experiments (Walsh and Legendre 1982, 1986; Queguinger and Legendre, 1986). It was suggested that the photosynthetic responses of algae depend on whether the irradiance fluctuated between limiting and saturated region (Walsh and Legendre, 1982). More research is needed to better understand the impact of short-term light fluctuations on phytoplankton photosynthetic rates. Also, to our knowledge the influence of light fluctuations on other photochemical processes in the ocean involving either organic or inorganic molecules (e.g. Millero, 1996) has not been investigated yet.

The goal of this study is to improve the understanding of short-term variability of the light field in the ocean. Toward this goal we report concurrent high temporal resolution measurements of spectral downwelling irradiance and upwelling radiance at 15 and 35 m depths in the Sargasso Sea. By performing time-series analysis, we examine typical examples of short-term variability of the light field in clear oligotrophic waters. This new data set is unique, because even if a number of experimental and theoretical attempts were made in the past to investigate short-term variations of the light field in the ocean (e.g. Walker, 1994), most of them were limited to the observations of a single optical parameter, i.e. downwelling irradiance in a single wavelength band.

2. Methods

The characterization of the short-term variability is still seriously limited, because optical measurements have been typically made by instruments lowered from ships. Data obtained in such a way are limited in temporal resolution as well as by errors due to ship movements and shadowing. Our measurements were made from a fixed position mooring, which allowed us to collect high-quality time-series data, suitable to study temporal variability of the optical signals. More details about the methods and data sets collected during deployment of the mooring are given elsewhere (Stramska and Frye, 1997), and only a brief summary will be given here. One of the priorities of the mooring program is to collect optical time series that can be compared with satellite ocean color data products, but the sampling procedures have been designed to insure the production of a variety of scientific products. The mooring was located

about 80 km southeast off Bermuda in waters of ~ 4570 m depth and included the following instrumentation:

- *On the surface buoy*: Instruments to measure wind speed and direction and air temperature (Coastal Climate), spectral downwelling irradiance (Satlantic), downwelling broadband irradiance PAR (400–700 nm, Li-Cor), and X and Y tilt sensors.
- *At 15 and 35 m depths*: Radiometer packages (MORS) with spectral downwelling irradiance and upwelled radiance sensors (Satlantic), scalar and downwelling PAR sensors (Li-cor), water temperature and pressure sensors (Sea-Bird).
- *At 20 and 80 m depths*: Bio-optical sensor packages (BIOPS), each with 9-wavelength absorption/attenuation meter (AC-9, WET Labs), stimulated fluorometer (SeaTech), and scalar PAR sensor (Biospherical).
- *At 45 and 65 m depths*: Multivariable moored systems (MVMS), each including a vector measuring current meter (VMCM), a thermistor for water temperature measurements, a scalar PAR sensor (Biospherical), a beam transmissometer (660 nm), and a stimulated fluorescence sensor (both from SeaTech).
- additionally there were three water temperature recorders (TPODS), at 55, 120 and 150 m depths, nitrate analyzers at 80 and 200 m depths, and S-4 current meters at 25 and 200 m depths.

The major focus of the present paper is on the data collected with spectroradiometers, which were located at 15 and 35 m depths. Instruments used for radiometric measurements were Satlantic radiometers OCI 100 and OCR-200, which comply with SeaWiFS requirements (Mueller and Austin, 1992). These radiometers measured downwelling irradiance (E_d) and upwelling radiance (L_u) at seven spectral bands with 10 nm bandwidths centered at 412, 443, 490, 510, 555, 665, and 683 nm. The size of the light collectors in the Satlantic radiometers is about 0.5 cm in diameter. Spectral E_d and L_u were measured at a rate of 6 Hz over 2 or 5-minute long intervals every hour during the daytime (from 0900 to 2300 GMT or 6 a.m. to 8 p.m. local summer time in Bermuda). For the evaluation of possible sensor drift, E_d and L_u were also sampled three times at night (at 0200, 0300 and 0400 GMT). Because of the limited memory of the data acquisition system, the 5 min E_d and L_u time series were collected only at 1400, 1500 and 1600 GMT (near solar noon). Water pressure and PAR were sampled once every hour over a sampling time of 5 min and at a rate of 6 Hz. The data were recorded with full frequency resolution using the internal hard drives of the *in situ* system and were downloaded after the recovery of the mooring. Time series analysis using algorithms described by Bendat and Piersol (1966) were performed. The power spectra of the data sets were obtained using a conventional Blackman–Tukey method with Parzen weighting function. The standard error is 26% in the power spectrum estimates presented below.

3. Results and discussion

An overview of the conditions at the mooring site during the 12 d long time period just after the mooring deployment is given in Figure 1. Time series of PAR at 20 m

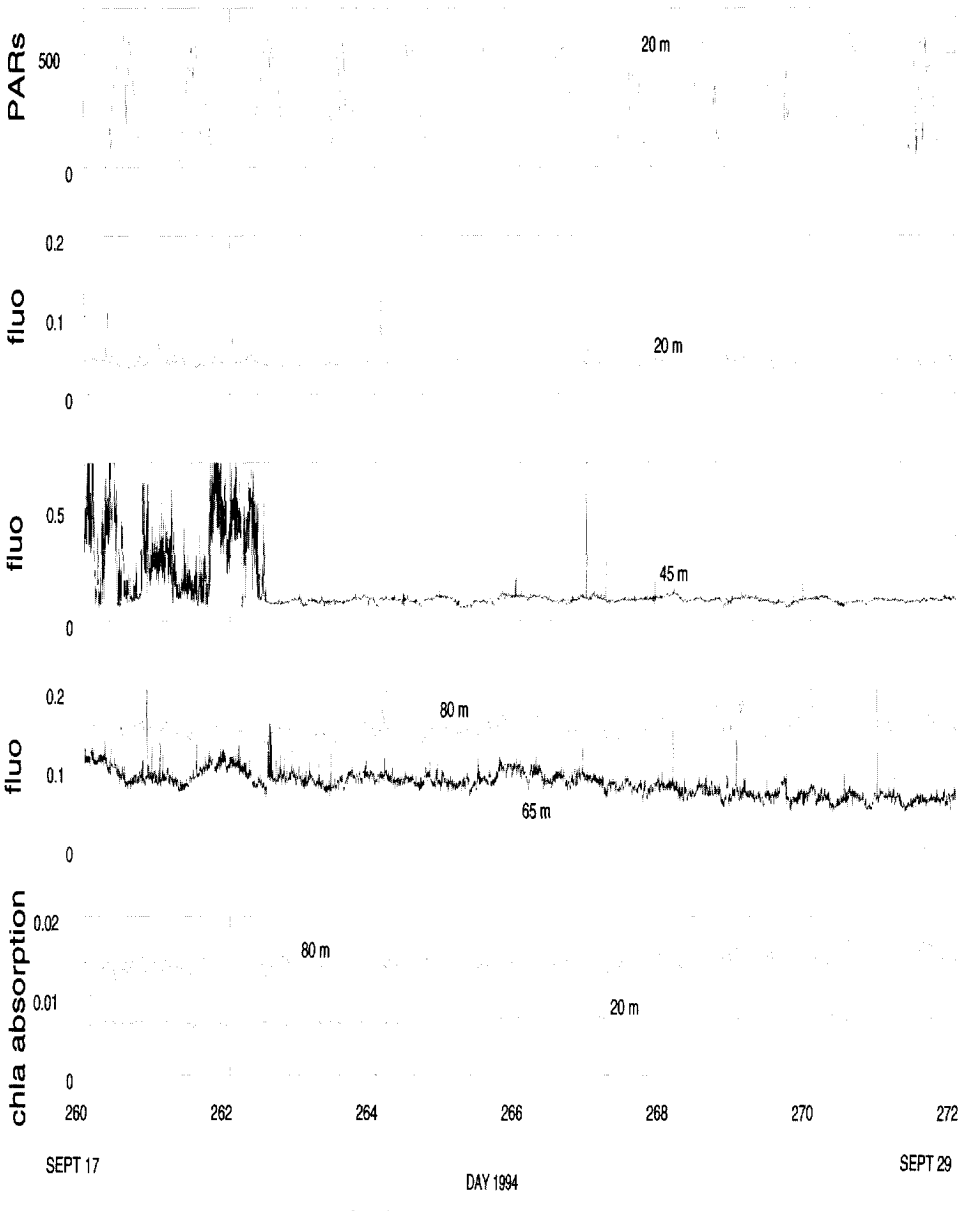

Fig. 1. Time series of PAR (μEinst $m^{-2} s^{-1}$) at 20 m depth, stimulated fluorescence (fluo, mg Chl a m^{-3}) at 20, 45, 65, and 80 m depths, and chlorophyll absorption (m^{-1}) at 20 and 80 m depths. Chlorophyll absorption was estimated from AC-9 data using the following expression: $a_{chl} = (a_{676} - a_{w676}) - (a_{715} - a_{w715})$, where a_{676} and a_{715} are the absorption coefficients at 676 and 715 nm, and a_w is the absorption of pure water.

depth recorded by MVMS with 4 min temporal resolution are shown at the top panel of Fig. 1. The optical data from day 264 (September 21) will be discussed in greater detail in this paper to show characteristic examples of short-term variability of underwater light field. Time series of PAR recorded at 20 m depth during day 264 indicate that we observed clear sky conditions during the first half of the day, followed by overcast conditions in the afternoon. Time series of stimulated fluorescence and chlorophyll absorption shown in Fig. 1 indicate low, almost constant concentration of chlorophyll-like pigments in surface waters over the time period of several days including day 264 (September 21). The vertical attenuation coefficient (K_d) calculated from spectral downwelling irradiance recorded at 15 and 35 m depths was quite low: for example, K_d at 490 and 510 nm was equal to 0.026 and 0.04 m^{-1}, (Stramska and Frye, 1997). Thus, our data represent very clear water conditions. Winds were weak and moderate (< 7 m s^{-1}) and we observed relatively strong thermal stratification of the water column.

Downwelling irradiance (PAR) and water pressure time series recorded on September 21 by the MORS located at 15 m depth are shown in Fig. 2. Each group of data points represents 5 min time series data collected every hour from sunrise to sunset.

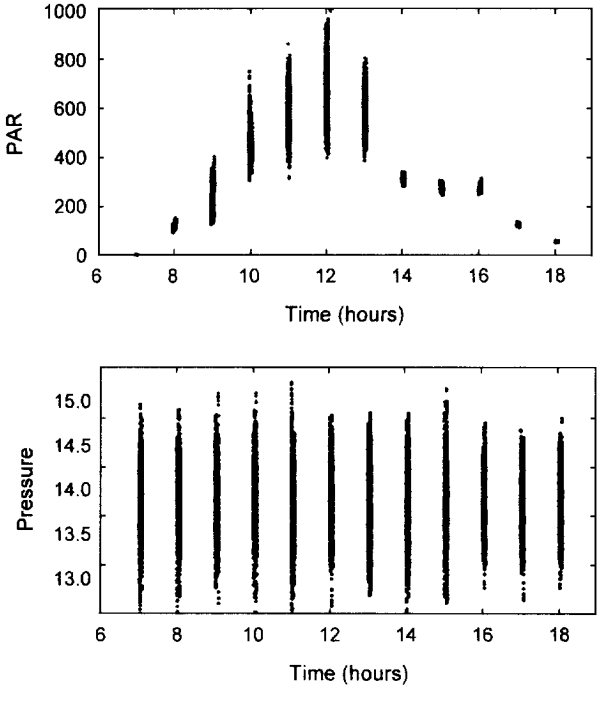

Fig. 2. Downwelling irradiance (PAR, in μEinst m^{-2} s^{-1}) and water pressure (in meters of water) recorded near Bermuda at 15 m depth on 21 September, 1994. Each group of points represents 5 min time series of data collected every hour.

Visual inspection of the data indicates that while the amplitude of the water pressure variability remained approximately unchanged during the day, the amplitude of downwelling PAR fluctuations changed dramatically. Comparison with time series shown in Fig. 1 (and also with the PAR data from the surface buoy, not shown here) indicates that the large amplitude of the in-water PAR was recorded under clear sky conditions, while the smaller amplitude corresponded to the situation when the sky was covered by clouds.

Subsets (100 s long) of time series of PAR and water pressure measured under clear and cloudy sky conditions are shown in Fig. 3a and b. Note that the time series shown in Fig. 3a were collected approximately 1 h before local solar noon (at 12 local summer time, see Fig. 2), and data shown in Fig. 3b were collected approximately 1 h after local solar noon (at 14 local summer time, see Fig. 2); therefore the difference in the solar altitude between the two data subsets was not significant ($\sim 4°$). The distinct features of PAR variability in Fig. 3a and b are quite obvious. Under cloudy sky conditions, water pressure and PAR time-series track each other closely, with the maxima of PAR corresponding to the minima in water pressure (Fig. 3b). This suggests that the effects of the variable path of light from sea surface to the light collector were dominant during this time. Changes in the length of this path can be attributed to significant surface waves. In contrast, under clear sky conditions (Fig. 3a) the PAR signal is characterized by variability occurring on a shorter time scale than the dominant frequency in the water pressure signal. As was shown in Fig. 1, fluorescence and chlorophyll absorption data (as well as other radiometric and beam attenuation data, not shown here for brevity) indicate that the transparency of the water column remained unchanged during this day. Because solar altitude, water transparency, and water pressure variability remained virtually unchanged during this time period, the differences in the observed pattern of the underwater light variability may be attributed to changes in the sky conditions.

In order to quantitatively examine the frequency distribution of the variance of the time series data, estimates of power spectral density were calculated. The results of these calculations for the spectral downwelling irradiance (E_d, dash-dot-dot line) and upwelling radiance (L_u, dash-dot line) measured at 15 m depth under clear sky conditions are shown in Fig. 4. The power spectrum for concurrently measured water pressure is also included in each plot (dotted line). To facilitate the comparison, the power spectra were normalized by the total variance. The estimates presented in Fig. 4 correspond to the time series shown in Fig. 3a. It is important to note that the shape of the power spectra for E_d and L_u in the blue/green part of the light spectrum (412, 443, 490, 510, and 555 nm) is similar for the five cases presented in Fig 4. In contrast, the shape of power spectra at 665 and 683 nm is quite different from that observed for shorter wavelengths.

We first discuss the results of our calculations for the blue/green light wavelengths (i.e. 412, 443, 490, 510, and 555 nm). Note that there is a significant shift in the dominant frequency in the E_d and L_u power spectra towards higher frequencies if compared to the position of the peak in the power spectrum of water pressure. This indicates that the majority of the variance in the irradiance and radiance can be attributed to the focusing of light by surface waves associated with fluctuations in

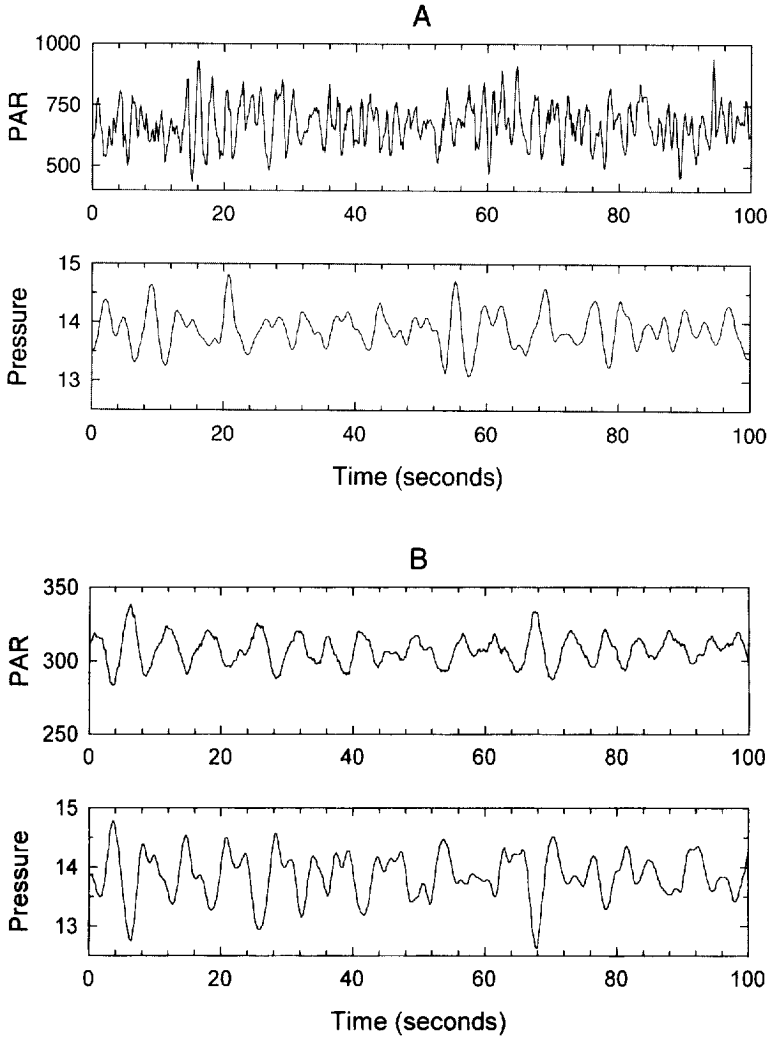

Fig. 3. Time series of downwelling irradiance (PAR, in μEinst m^{-2} s^{-1}) and water pressure (in meters of water) recorded at 15 m depth on 21, September 1994: (a) under clear sky conditions; (b) under cloudy sky conditions.

Fig. 4. Power spectral density (G_x) of downwelling irradiance (dash-dot-dot) and upwelling radiance (dash-dot) measured at 15 m depth under clear sky conditions. Plots are for 412, 443, 490, 510, 555, 665, and 683 nm. For comparison the power spectrum for water pressure is included on each plot (dotted line). All power spectra were normalized to the total variance.

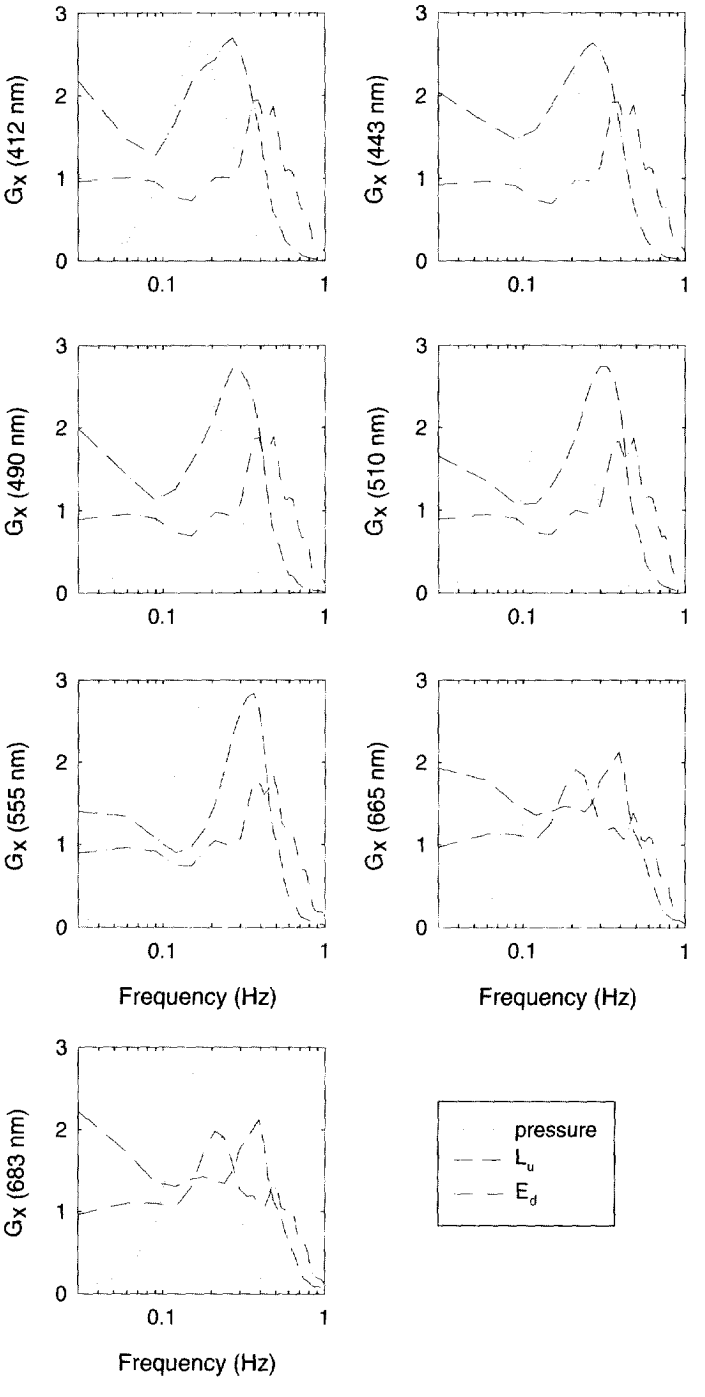
Gx (412 nm)
Gx (443 nm)
Gx (490 nm)
Gx (510 nm)
Gx (555 nm)
Gx (665 nm)
Gx (683 nm)
0
1
2
3
0.1
1
Frequency (Hz)
pressure
L_u
E_d

surface curvature and slopes and not with fluctuations in the water column height. However, this shift in frequency is smaller for the upwelling radiance than for the downwelling irradiance. In addition, while the maxima of the power spectra for E_d at 412, 443, 490, 510, and 555 nm cover approximately the same frequency band, the width of the corresponding peaks of the power spectra for L_u decreases progressively from short to longer wavelengths (the widest for L_u at 412 nm and the narrowest for L_u at 555 nm).

An apparent reason for the difference in the general features of the power spectra of E_d and L_u follows. The upward light flux can be regarded as the fraction of the downward flux, which has been scattered upward. Therefore, because upwelling light is less directional and more diffuse than the downwelling light at the same water depth, we expect that the upwelling light should be much less affected by the wave focusing phenomenon than the downwelling light. Furthermore, in very clear water the light at shorter wavelengths is much more effectively scattered than the light at longer wavelengths. This is due to the fact that the wavelength dependence of molecular scattering follows a power law with the exponent of -4.32 (e.g. Kirk, 1994). Because of this and the spectral shape of the absorption of clear oceanic water, the scattering to absorption ratio strongly decreases with light wavelength. The angular distribution of light is determined by the relative importance of scattering and absorption processes; therefore, at a given water depth the light at shorter wavelengths becomes more diffuse and less affected by the wave focusing phenomenon than light at longer wavelengths. This is supported by the calculated coefficient of variation for E_d and L_u fluctuations for each of the measured time series of E_d and L_u. The coefficient of variation is defined here as the ratio of the standard deviation to the mean value of the relevant time series. The results of the calculations summarized in Table 1 indicate, for example, that the coefficient of variation increased from about 13% for E_d at 412 to 17.5% at 555 nm for the 15 m depth at noon time. The coefficient of variation for L_u was much smaller than that for E_d, and it varied between 4.5% at 412 nm and 8.7% at 555 nm.

As mentioned above, the shape of the power spectral density for the red light displayed different features than for shorter wavelengths. At 665 and 683 nm the most important component in the variability of E_d is close to the frequency of the dominant peak of the power spectrum for water pressure, indicating that the changes of the water column depth were affecting the variability of E_d at 665 and 683 nm more than at shorter wavelengths. On the other hand, the power spectra of L_u at 665 and 683 nm have maxima at approximately the same frequency as the power spectra of E_d at shorter wavelengths. Thus, the light field at red wavelengths responds in a different way to surface waves than light at shorter wavelengths. This can be explained in the following way. First, the red light is characterized by relatively high absorption by water. Photons of red light, which, due to refraction at the air–water interface, travel less vertically, have greater effective pathlength when they penetrate to a given water depth and therefore have a greater probability of being absorbed than the light traveling vertically. This is probably why we observed that E_d values at 665 and 683 nm were more affected by changes in water column height and less influenced by the wave focusing than E_d at blue/green wavelengths. Second, another factor to be

considered is the red light generated at depth by inelastic scattering processes such as phytoplankton fluorescence (e.g. Kiefer et al., 1989; Chamberlin et al., 1990) and Raman scattering. The fluoresced light is nearly uniform directionally, and although it is too weak to be detected in the downwelling light stream close to the water surface, it usually shows up as a distinct peak in the spectral distribution of the upwelling light and ocean surface reflectance. Raman scattered photons have also nearly uniform angular distribution and contribute to the light field in the red portion of the spectrum. Therefore, it is likely that at the 15 m depth most of the upwelling radiance at 665 and 683 nm is attributed to inelastic scattering of light. Consequently, temporal changes in L_u at 665 and 683 nm are largely determined by fluctuations of light at shorter wavelengths that excite phytoplankton fluorescence and Raman scattering.

Next we examine power spectra calculated for E_d and L_u measured at 35 m depth (Fig. 5). These time series were also obtained under clear sky conditions, concurrently with time series analyzed in Figure 4. We first consider the results for the blue/green light. Note that the coefficients of variation of E_d and L_u at 35 m depth are much smaller than at 15 m depth (Table 1), which indicates that the importance of the wave focusing effect decreases with water depth, as expected. However, power spectra of E_d and L_u exhibit distinct maxima and, similarly to the 15 m depth, we observe a shift of the dominant peak in the power spectra of E_d and L_u towards higher frequencies as compared to the dominant peak in the power spectrum of the water pressure. Note that this shift is smaller and there is much less contribution to the variance of E_d at the high-frequency band than at 15 m depth (Fig. 4). This can be explained by geometrical models of the focusing effect, indicating that short surface waves have their point of maximum focus at a shorter distance from the sea surface than longer waves (Schenck, 1957; Snyder and Dera,1970; Stramski and Dera, 1988). Therefore, higher-frequency components of irradiance fluctuations are rapidly damped with depth, causing a narrowing of the power spectra of irradiance.

Again a different pattern emerges when we analyze the power spectra for E_d and L_u at 665 and 683 nm. At red wavelengths power spectra of both E_d and L_u have their maxima at approximately the same frequency as the maxima of E_d power spectra in the blue/green. This is due to the fact that strong absorption of red light by water effectively removes sunlight at the red end of the light spectrum. We expect that at 35 m depth both the downwelling and upwelling light fields in the red are dominated by natural fluorescence of phytoplankton and Raman scattered photons. In turn, fluorescence intensity and Raman scattered intensity follow fluctuations of light that excites these inelastic processes, that is, largely fluctuations in downwelling irradiance at excitation (blue) wavelengths. Note also that the coefficient of variation for L_u at 665 and 683 nm is significantly larger than that for L_u at shorter wavelengths (Table 1).

We will now consider power spectra for E_d, L_u, and water pressure under cloudy sky conditions at 15 and 35 m depths. These power spectra are plotted in Figs. 6 and 7 for 15 and 35 m depth. The maxima in the power spectra for E_d and L_u are approximately at the same frequency range as the maxima in the power spectra of water pressure. This indicates that under cloudy sky conditions the majority of the

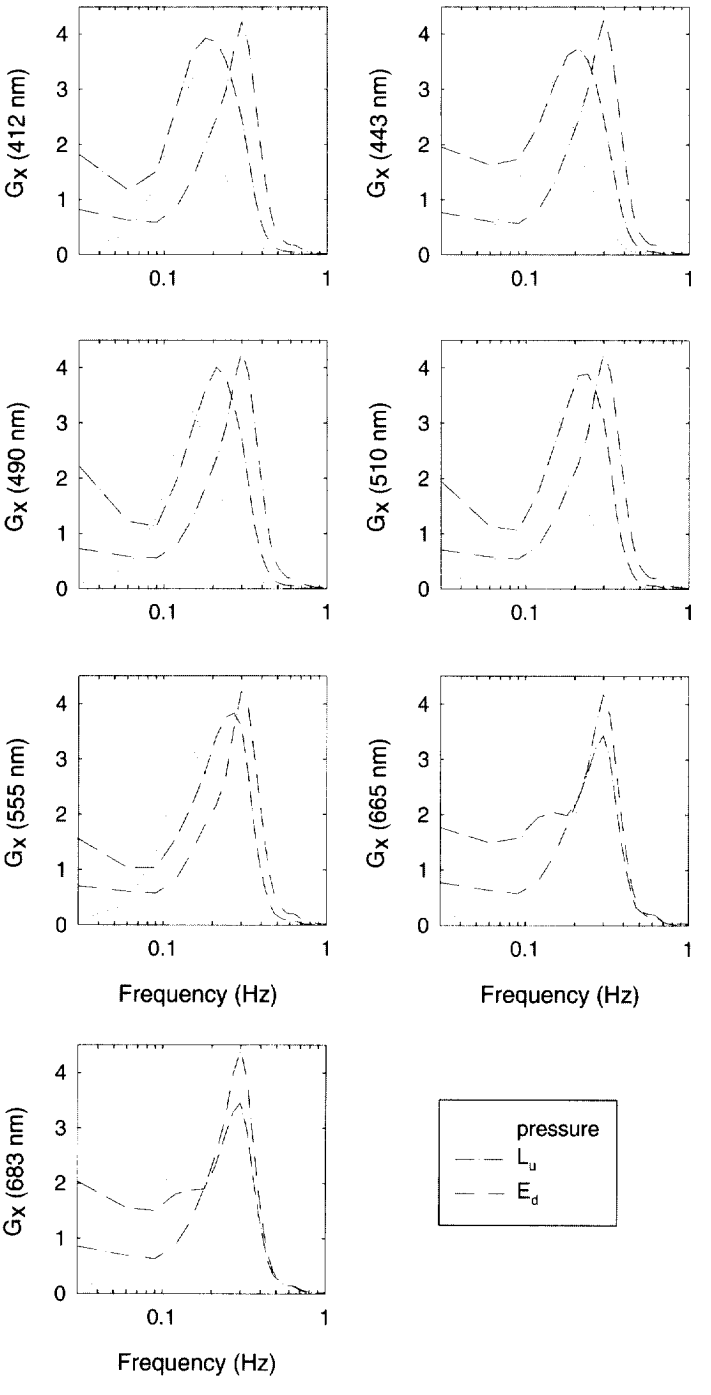
Gx (412 nm)
Gx (443 nm)
Gx (490 nm)
Gx (510 nm)
Gx (555 nm)
Gx (665 nm)
Gx (683 nm)
0
1
2
3
4
0.1
1
Frequency (Hz)
pressure
L_u
E_d

Table 1
Calculated coefficient of variation (%) of spectral downwelling irradiance (E_d) and upwelling radiance (L_u). The coefficient of variation is defined here as the ratio of the standard deviation to the mean value of the relevant time series

	15 m at noon	35 m at noon	15 m at 2 p.m.	35 m at 2 p.m.
E_d (412 nm)	13.1%	8.0%	2.6%	1.7%
E_d (443 nm)	14.5%	9.0%	2.7%	1.7%
E_d (490 nm)	16.0%	10.2%	2.8%	1.8%
E_d (510 nm)	16.6%	11.0%	3.1%	2.2%
E_d (555 nm)	17.5%	12.0%	3.5%	2.9%
E_d (665 nm)	19.4%	10.1%	8.1%	7.5%
E_d (683 nm)	19.5%	9.4%	8.5%	4.4%
L_u (412 nm)	4.5%	4.8%	2.1%	2.7%
L_u (443 nm)	4.8%	4.9%	2.0%	2.4%
L_u (490 nm)	5.5%	5.2%	2.0%	2.1%
L_u (510 nm)	6.6%	5.7%	2.3%	2.2%
L_u (555 nm)	8.7%	6.8%	2.8%	2.4%
L_u (665 nm)	13.1%	10.2%	3.4%	3.0%
L_u (683 nm)	13.1%	9.6%	3.2%	2.0%

variance of E_d and L_u can be explained by the variations in the water pressure, which is a measure of the water column height above the light collector. These wave-induced fluctuations for cloudy skies have much smaller amplitudes than fluctuations for clear skies (see Table 1).

It has been previously reported that the frequency and intensities of underwater light fluctuations are dependent on sky conditions and sea-surface state. The most favorable conditions for light focusing by waves prevail when winds are moderate (2–5 m s^{-1}), sun elevation is more than 40°, and diffuseness of surface irradiance is less than 40% (e.g. Dera and Stramski, 1986; Dera et al., 1992). These previous experiments showed that decreasing sun altitude, increasing atmospheric diffuseness, sea surface roughness, and water turbidity act to reduce the frequency and intensity of light fluctuations. This has also been explained by models of the focusing effect, which indicate that focusing is most efficient for a collimated light beam (e.g. Snyder and Dera, 1970). Although we do not have any information regarding irradiance diffuseness at the sea surface, it seems that our clear sky data represent quite favorable conditions for the formation of the focusing effects, because the in-water vertical attenuation coefficient was rather low (0.026 and 0.04 at 490 and 510 nm, respectively), and sun elevation was quite high (about 60°). Wind speed was only slightly higher

Fig. 5. Power spectral density (G_x) of downwelling irradiance (dash-dot-dot) and upwelling radiance (dash-dot) measured at 35 m depth under clear sky conditions. Plots are for 412, 443, 490, 510, 555, 665, and 683 nm. For comparison the power spectrum for water pressure is included on each plot (dotted line). All power spectra were normalized to the total variance.

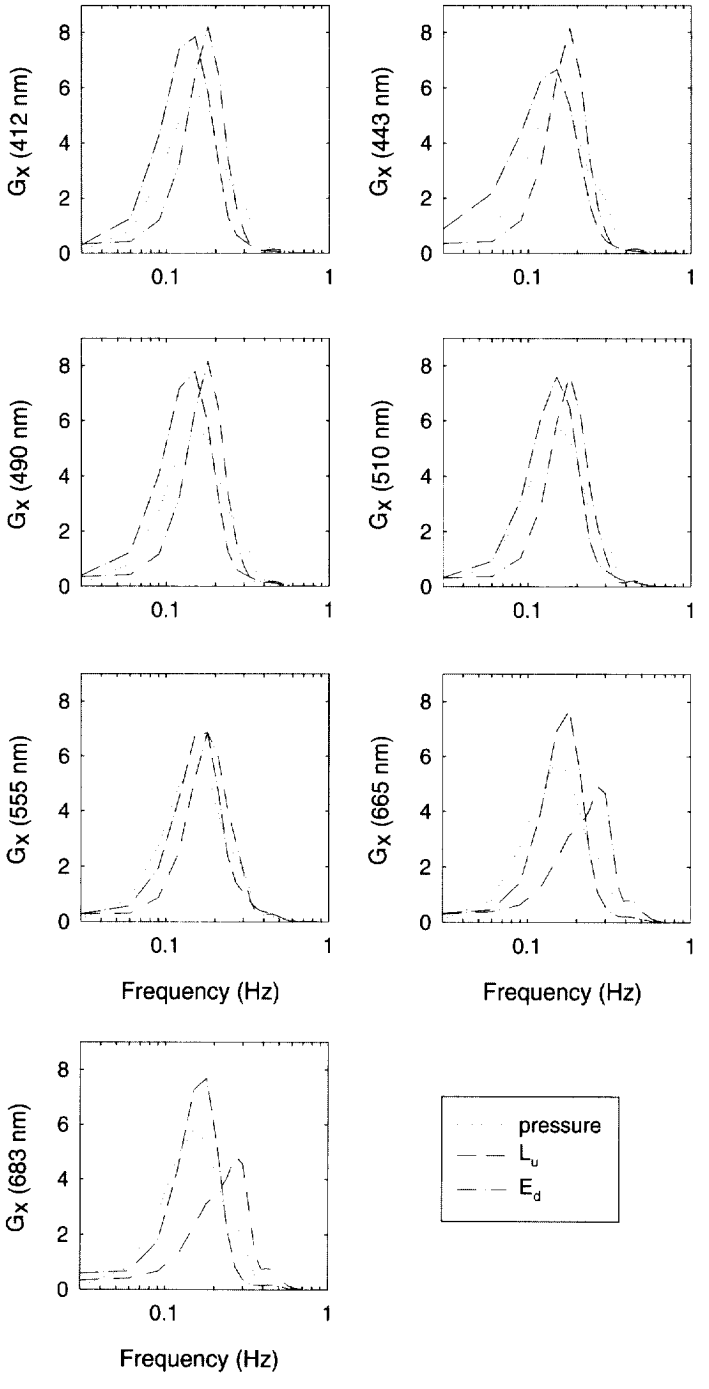
Gx (412 nm)
Gx (443 nm)
Gx (490 nm)
Gx (510 nm)
Gx (555 nm)
Gx (665 nm)
Gx (683 nm)
0
2
4
6
8
0.1
1
Frequency (Hz)
pressure
L_u
E_d

than optimal, about 7 m s^{-1}. Note, however, that because we did not measure parameters that fully describe sky and sea surface conditions (e.g. irradiance diffuseness, surface curvature, high frequency surface wave spectra), we cannot quantify influence of these conditions on the underwater light field variability. Note also that a full description of the underwater light field fluctuations will be possible only when appropriate data are collected with greater vertical resolution, as the intensity of light focusing effects decreases rapidly with depth (e.g. Dera and Stramski, 1986; Stramski and Dera, 1988). Therefore, our results should be treated as a preliminary illustration of the distinctive patterns of the light field variability under clear and cloudy sky conditions.

In summary, our data enable us to make several conclusions about short-term variability of the light field in the oligotrophic ocean. First, under clear sky conditions wave focusing effects dominate light variability in the upper part of the water column, as we observed these effects at 35 m depth. Since it has been estimated that more than half of the integrated primary production in this region occurs at depths less than 39 m (Siegel et al., 1995), light fluctuations may be of ecological significance. Second, light focusing effects were stronger at shallower water depth and more pronounced for the downwelling light than for the upwelling light. Third, our results indicate that the effects of light focusing depend on light wavelength. This was documented by the changes in the coefficient of variation, which, for both E_d and L_u, increased with light wavelength, and also by the changes in the shape of power spectra for L_u. The general trends presented above can be explained by the wavelength dependency of the angular structure and efficiency of attenuation of light. Fourth, the most striking results of this work involve the differences between the characteristics of light fluctuations at the red wavelengths in comparison to the shorter wavelengths. For example, the coefficients of variation for L_u at 665 and 683 nm were more than twice as high as those for the blue wavelengths. Also the shape of the power spectra for L_u at 665 and 683 nm was not similar to the shape of power spectra for L_u at shorter wavelengths but displayed dominant peaks located at the same frequency as the maxima in the power spectra for E_d at the blue/green wavelengths. This implies that at the depths of our measurements light fluctuations in the red can be attributed to inelastically scattered radiation from phytoplankton fluorescence and Raman scattering, which was responding to fluctuations of light at shorter excitation wavelengths.

Acknowledgements

This work was supported by NASA grant NAGW-3949 and NSF Oceanographic Technology and Interdisciplinary Coordination Program grant OCE-9415667

Fig. 6. Power spectral density (G_x) of downwelling irradiance (dash-dot-dot) and upwelling radiance (dash-dot) measured at 15 m depth under cloudy sky conditions. Plots are for 412, 443, 490, 510, 555, 665, and 683 nm. For comparison the power spectrum for water pressure is included on each plot (dotted line). All power spectra were normalized to the total variance.

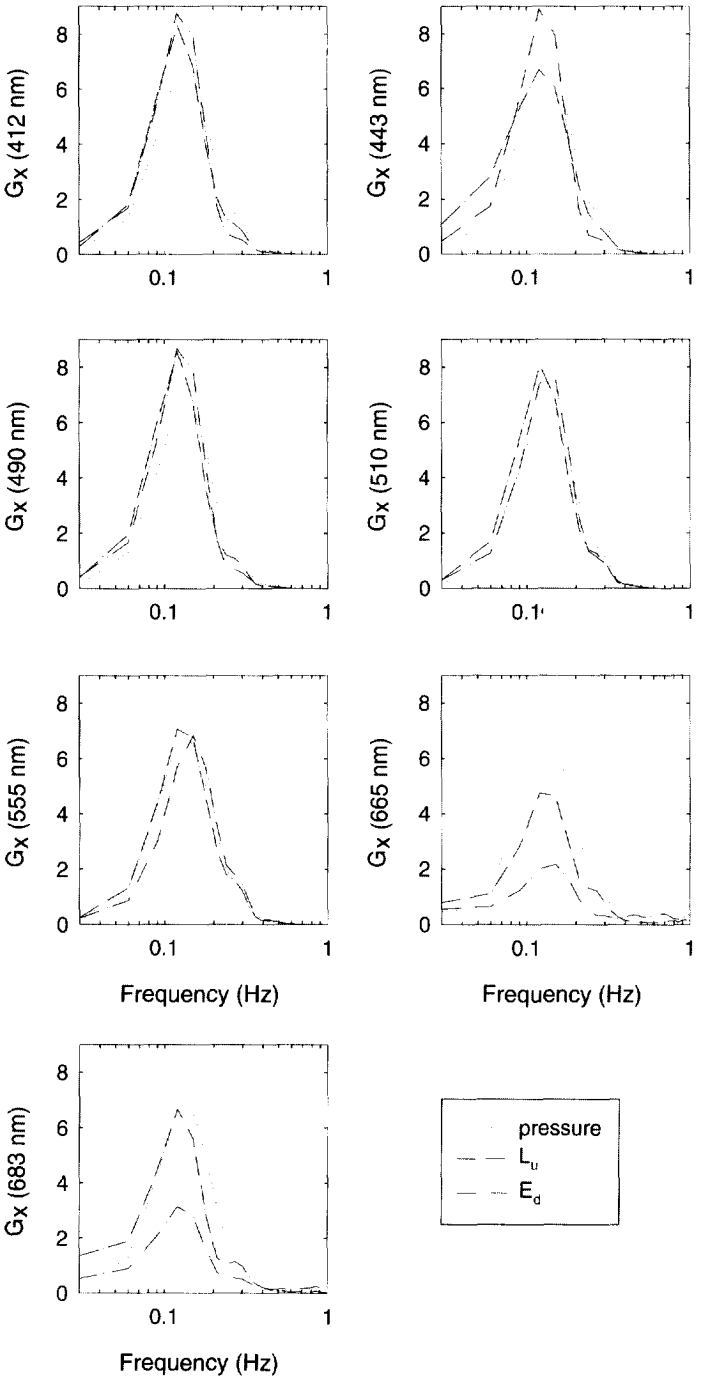
Gx (412 nm)
Gx (443 nm)
Gx (490 nm)
Gx (510 nm)
Gx (555 nm)
Gx (665 nm)
Gx (683 nm)
0
2
4
6
8
0.1
1
Frequency (Hz)
pressure
L_u
E_d

awarded to the authors. The mooring hardware and telemetry has been funded by ONR Contract N00014-94-1-0346 to Dan Frye. We thank colleagues from the Ocean Physics Group USC and BATS program for their outstanding dedication to collecting the data presented here. Special thanks are due to Derek Manov, Liz Caporelli, and Isabelle Taupier-Letage for their assistance with many aspects of the field work. We also thank the WHOI team led by John Kemp and the crew, marine technicians and master of the Weatherbird II for their commitment to the mooring operations.

References

Abbott, M.R., Richerson, P.J., Powell, T.M. 1982. In situ response of phytoplankton fluorescence to rapid variations in light. Limnology and Oceanography 27, 218–225.

Bendat, J.S., Piersol, A.G., 1966. Measurements and Analysis of Random Data. Wiley, New York, 390pp.

Bishop, J.K.B., Rossow, W.B., 1991. Spatial and temporal variability of global surface solar irradiance. Journal of Geophysical Research 96, 16839–16858.

Chamberlin, W.S. et al., 1990. Evidence for a simple relationship between natural fluorescence, photosynthesis and chlorophyll in the sea. Deep-Sea Research Part A 37, 951–973.

Dera, J., Gordon, H., 1968. Light field fluctuations in the photic zone. Limnology and Oceanography 13, 697–699.

Dera, J., Sagan, S., Stramski, D., 1992. Focusing of sunlight by sea surface waves: new measurement results from the Baltic Sea. Optics of the Air-Sea Interface, SPIE Proceedings 1749, 65–72.

Dera, J., Stramski, D., 1986. Maximum effects of sunlight focusing under a wind-disturbed sea surface. Oceanologia 23, 15–42.

Dera, J. et al., 1975. Fluctuation of light in the euphotic zone and its influence on primary production. Merentutkimuslaitoksen Julk 239, 351–364.

Gallegos, C.L., Hornberger, G.M., Kelly, M.G., 1980. Photosynthesis-light relationships of a mixed culture of phytoplankton in fluctuating light. Limnology and Oceanography 25, 1082–1092.

Gross, L.J., 1982. Photosynthetic dynamics in varying light environments: A model and its application to whole leaf carbon gain. Ecology 63, 84–93.

Gross, L.J., Chabot, B.F., 1979. Time course of photosynthetic response to changes in incident light energy. Plant Physiology 63, 1033–1038.

Kirk, J.T.O., 1994. Light and photosynthesis in Aquatic Ecosystems. Cambridge University Press, Cambridge, U.K., 509pp.

Kiefer, D.A., Chamberlin, W.S., Booth, C.R., 1989. Natural fluorescence of chlorophyll a: Relationship to photosynthesis and chlorophyll concentration in the western South Pacific gyre. Limnology and Oceanography 34, 868–881.

Fig. 7. Power spectral density (G_x) of downwelling irradiance (dash-dot-dot) and upwelling radiance (dash-dot) measured at 35 m depth under cloudy sky conditions. Plots are for 412, 443, 490, 510, 555, 665, and 683 nm. For comparison the power spectrum for water pressure is included on each plot (dotted line). All power spectra were normalized to the total variance.

Nikolaev V.P. et al., 1972. Statistical characteristics of underwater illumination Fizika Atmosfery i Okeana 8, 936–944 (in Russian).

Marra, J., 1978. Effects of short-term variations in light intensity on photosynthesis of a marine phytoplankter: a laboratory study. Marine Biology 46, 191–202.

Marra, J., Heinemann, K., 1982. Photosynthesis response by phytoplankton to sunlight variability. Limnology and Oceanography 27, 1141–1153.

Millero, F.J., 1996. Chemical Oceanography, CRC Press, Boca Raton, FC, 469pp.

Mueller, J.L., Austin, R.W., 1992. Ocean optics protocols. In: Hooker, S.B., Firestone, E.R. (Eds.), NASA Tech. Memo. 104566, vol. 5, 45pp.

Queguiner, B., Legendre, L., 1986. Phytoplankton photosynthetic adaptation to high frequency light fluctuations simulating those induced by sea-surface waves. Marine Biology 90, 483–491.

Schenck, H., Jr., 1957. On the focusing of sunlight by ocean waves. Journal of the Optical Society of America 47, 653–657.

Siegel, D.A., Michaels, A.F., Sorensen, J.C., O'Brien, M.C., Hammer, M.A., 1995. Seasonal variability of light utilization in the Sargasso Sea. Journal of Geophysical Research, 100(8), 695–713.

Snyder, R.L., Dera, J., 1970. Wave-induced light-field fluctuations in the sea. Journal of the Optical Society of America 6, 1072–1079.

Stramski, D., Booth, C.R., Mitchell, B.G., 1992. Estimation of downward irradiance attenuation from a single moored instrument. Deep-Sea Research 39, 567–584.

Stramski, D., Dera, J., 1988. On the mechanism for producing flashing light under a wind disturbed water surface. Oceanologia 25, 5–21.

Stramska, M., Frye, D., 1997. Dependence of apparent optical properties on solar altitude: Experimental results based on mooring data collected in the Sargasso Sea. Journal of Geophysical Research 102(15), 679–691.

Sudbin, A.I., Pelevin, V.N., Shifrin, K.S., 1974. Fluctuations of underwater irradiance. Monin, A.S., Shifrin, K.S. In: (Eds.), Hydrophysical and Hydrooptical Investigations in the Atlantic and Pacific Ocean. Nauka, Moskva, pp. 202–213.

Thornley, J.H.M., 1974. Light fluctuations and photosynthesis. Annals of Botany 38, 363–373.

Walker, R.E., 1994. Marine Light Field Statistics. Wiley, New York, 675pp.

Walsh, P., Legendre, L., 1982. Effects des fluctuations rapides de la lumiere sur la photosynthese du phytoplancton. Journal of Plankton Research 4, 313–327.

Walsh, P., Legendre, L., 1986. Photosynthetic responses of the diatom Phaeodactylum tricornutum to high frequency light fluctuations simulating those induced by sea surface waves. Journal of Plankton Research 10, 1077–1082.

Weidemann, A. et al., 1990. Calculation of near-surface attenuation coefficients: the influence of wave focusing. Ocean Optics X, SPIE Proceedings 1302, 492–504.